ISSN:1991-8178

Australian Journal of Basic and Applied Sciences

Journal home page: www.ajbasweb.com

Numerical Modeling For Gravity Waves Over Submerged Porous Media

[1]I. Magdalena and[2]S.R. Pudjaprasetya

[1,2]Industrial & Financial Mathematics Research Group, Fac. of Mathematics and Natural Sciences, InstitutTeknologi Bandung,JalanGanesha 10, Bandung, West Java, Indonesia

ARTICLE INFO

Article history:
Received 23 June 2015
Accepted 25 July 2015
Available online 30 August 2015

Keywords:
submerged porous media; two-layer shallow water equation; hydrodynamic pressure; staggered finite volume.

ABSTRACT

A numerical technique is presented here to solve free surface flow over submerged porous media. The governing equations used are the two-layer shallow water model. For flow in a submerged porous medium, Darcy resistance is included in the momentum equation. The staggered conservative scheme is implemented to solve the equations. Numerical simulation of an incoming wave over porous media shows dissipative mechanism that confirm the analytical damping. The experiment of standing waves dissipate over a submerged porous media as recorded in Ref. 5 and is used to validate our hydrodynamic scheme. The comparison shows that our numerical standing wave propagates with the correct speed, and thus confirm our hydrodynamic scheme.

ToCiteThisArticle:I. Magdalena and S.R. Pudjaprasetya., Numerical Modeling For Gravity Waves Over Submerged Porous Media. ***Aust. J. Basic & Appl. Sci.,****9(28): 124-130, 2015*

INTRODUCTION

The use of submerged porous breakwaters for coastal protections has increased in recent years. Reefball as an artificial reef is a submerged porous structure that was developed to provide beach protection with higher aesthetic appeal. As a breakwater, the porous structure can absorb and dissipate the energy of incoming waves.

This research presents a numerical techniques for wave propagation that passes overa submerged porous media and undergoes amplitude reduction. In this paper, we focus on developing a numerical method for simulating gravity waves over a submerged porous medium. C.P. Tsai in (Tsai, C.,*et al*., 2006) presented a new mild-slope equation to investigate the wave transformation over a submerged permeable breakwater on a variable permeable bottom topography. K.D. Do and Kyung-Duck Suhin derived damping rate by using the extended mild-slope equation to calculate wave dissipation over the permeable bed. Cruz et.al. in (1997) investigated wave transformation on porous bed by usingBoussinesq equations. O. Nwoguand Z. Demirbilekin (2006) developed a coupled Boussinesq and solve the equation by using boundary integral method to simulate nonlinear water wave interaction with structures consisting of multiple porous layers with different physical and hydraulic characteristics. The governing equation used in this paper is the two-layer shallow water model, in which the momentum equation for flow in a submerged porous medium adopts Darcy frictional force. Considering the shallow water equations as a hyperbolic system of conservation laws, the appropriate numerical method is the finite volume method. Here we implement the finite volume method on a staggered grid. This method is relatively simple to implement and to adjust for various fluid flow problems, see (Pudjaprasetya, S., and I. Magdalena, 2014; Magdalena, I.,*et al*.,). Moreover, this method is explicit, efficient and robust, see Ref. (Stelling, G., and S. Duinmeijer, 2003).

Some literatures such as (Stelling, G., and M. Zijlema, 2003; Zijlema, M., and G. Stelling, 2008; Casulli, V., 1999), and (Yamazaki, Y.,*et al*., 2011) enhance the above method to account for the vertical gradient of the hydrodynamic pressure using only a few vertical grid points. Following their approach, here we use two-layer formulation to resolve the vertical axis, one layer is for the upper ideal fluid, and the other is for fluid in the porous layer. Numerically, we solve the problem by decomposing the model, first by solving the hydrostatic model, and we then corrected it by taking into account the hydrodynamic terms. The resulting hydrodynamic scheme can simulate the propagation of a monochromatic wave over a submerged porous media, with wave attenuation that confirms the analytical damping. Moreover, our simulation of standing wave reducing over a submerged porous media confirms the experimental data by Z. Gu and H. Wang (Gu, Z., and H. Wang, 1991).

Corresponding Author: I. Magdalena, Industrial & Financial Mathematics Research Group, Fac. of Mathematics and Natural Sciences, InstitutTeknologi Bandung,JalanGanesha 10, Bandung, West Java, Indonesia
E-mail: ikha.magdalena@math.itb.ac.id

Two Layer Formulation For Wave Over A Porous Media:

In this section, the discretization used in this paper will be formulated. We consider the governing equations for two layer of fluid on a flat bottom. The equations are based on mass conservation and momentum balance for two layer of fluid with the same density with involving hydrodynamic pressure. Mass conservation for each layer are

$$(\eta - \eta_2)_t = -(hu)_t \quad (1)$$
$$\eta_{2_t} = -(HU)_x, \quad (2)$$

where $h = d_1 + \eta - \eta_2$ denotes the layer thickness for upper layer and $H = d_2 + \eta_2$ for lower layer. Notations η is surface elevation, $\eta_2$internal elevation, and d_k undisturbed water thickness for each layer. Horizontal velocity in x−directions for the upper and lower layer are denoted by u, U respectively. Index $k = 1$ is for the upper layer and $k = 2$ is the lower layer, see Figure 1.

Momentum balance in x-direction for each layer are

$$u_t + g\eta_x + uu_x = -\frac{1}{\rho}(P_1)_x, \quad (3)$$
$$+UU_x + \frac{1}{\rho_2}(\rho_1\, g\eta + (\rho_2 - \rho_1)\, g\eta_2)_x = -\frac{1}{\rho_2}(P_2)_x \quad (4)$$

where $P_k$with $k = 1,2$ represent the hydrodynamics pressure and ρ_k denotes density in each layer.

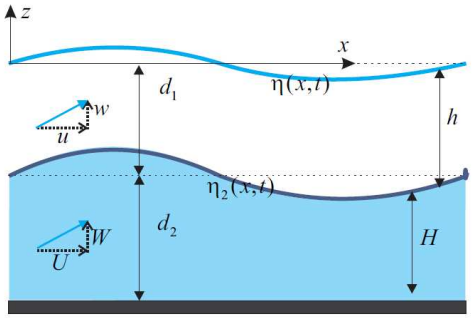

Fig. 1: Sketch of two layer fluid domain.

Compare to the well-known two layer model, Equations (2) and (4) get additional hydrodynamic terms. In order to complete this set of equations, we need to formulate momentum equation in z-direction and also linearized kinematic boundary condition:

$$w_t = -\frac{1}{\rho_1}(P_1)_z,$$
$$W_t = -\frac{1}{\rho_2}(P_2)_z,$$
$$\eta_t = w,$$
$$\eta_{2_t} = W,$$

respectively. Notation w,W denotes vertical velocity in z-directions. Three equations above are in linearized form. Moreover, mass conservation (1,2) in each layer can be combined to:

$$\eta_t + (hu)_x + (HU)_x = 0. \quad (9)$$

In this paper, we focus on the case where the lower layer is a porous medium and the density difference is assumed small enough $\rho_2 \simeq \rho_1 = \rho$. In this case, the two layer formulation above can be used with a modification in the momentum for the lower porous layer gets and additional resistance term. We model the resistance as a linear friction force using Darcy's Law $f\frac{\omega}{n}$ with f is the friction coefficient. Other modification is the fluid particle velocity (U,W) is replaced by the filtered velocity $\frac{1}{n}(U,W)$, where n is a porosity of the porous medium. The full governing equations is then read as

$$\eta_t + (hu)_x + \frac{1}{n}(HU)_x = 0, \quad (10)$$
$$u_t + g\eta_x + uu_x + \frac{1}{\rho}(P_1)_x = 0, \quad (11)$$
$$\frac{1}{n}U_t + g\eta_x + \frac{1}{n^2}UU_x + f\frac{\omega}{n}U + \frac{1}{\rho}(P_2)_x = 0,$$
$$w_t + \frac{1}{\rho}(P_1)_x = 0, \quad (13)$$
$$\frac{1}{n}W_t + \frac{1}{\rho}(P_2)_x = 0. \quad (14)$$

Recapitulating, the hydrodynamic two layer formulation of free surface flow over submerged porous media are equations (10-14).

Finite Volume Method on Staggered Grid:

In this section, we discuss the finite volume method implemented on a staggered grid to solve (10-14). First, in the subsection Hydrostatic Model we explain the approximation of the hydrostatic case and then in the subsection Hydrodynamic Pressure we discuss the correction due to the inclusion of dynamic pressure.

Hydrostatic Model:

Neglecting the effect of hydrodynamic pressure $P(x,z,t)$, the governing equationswithout advection terms are reduced to

$$\eta_t + (hu)_x + \frac{1}{n}(HU)_x = 0, \quad (15)$$
$$u_t + g\eta_x = 0, \quad (16)$$
$$\frac{1}{n}U_t + g\eta_x + f\frac{\omega}{n}U = 0 \quad (17)$$

(5)

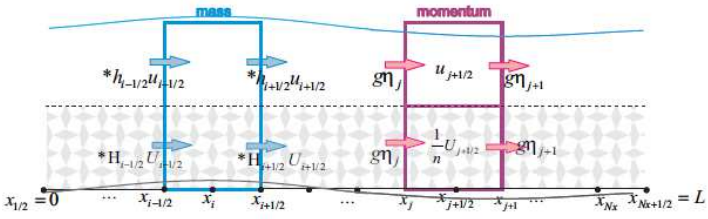

Fig. 2: Illustration of staggered grid with cell A_i for mass conservations and cells$C_{i+1/2}$ and $\bar{C}_{i+1/2}$ for momentum equations.

Consider a spatial domain [0,L] which is partitioned as $x_{1/2}=0, x_1, x_{\frac{3}{2}}, x_2, \ldots, x_{Nx}, x_{Nx+\frac{1}{2}}=L$. The staggered finite volume method means that equations are approximated on adjacent cells. Equation (15) is approximated at a cell $A_i=\left[x_{i-\frac{1}{2}}, x_{i+\frac{1}{2}}\right]\times[-d_2(x), \eta(x,t)]$, see Figure 2, whereas equations (16,17) are approximated at cell $\bar{C}_{i+1/2}=\left[x_j, x_{j+1}\right]\times[-d_1, \eta(x,t)]$ and $C_{i+1/2}=\left[x_j, x_{j+1}\right]\times[-d_2(x), -d_1]$, respectively.

Let we denote $q=hu$ and $H=QU$ mass flux along the upper and lower layer, respectively. The approximation for equations (15, 16, and 17) yield:

$$\frac{\eta_i^{n+1}-\eta_i^n}{\Delta t}+\frac{q_{i+1/2}^{n+1}-q_{i-1/2}^n}{\Delta t}+\frac{1}{n}\frac{Q_{i+1/2}^{n+1}-Q_{i-1/2}^n}{\Delta t}=0, \quad (18)$$

$$\frac{u_{i+\frac{1}{2}}^{n+1}-u_{i-\frac{1}{2}}^n}{\Delta t}+g\,\frac{\eta_{i+1}^{n+1}-\eta_i^{n+1}}{\Delta x}=0, \quad (19)$$

$$\frac{1}{n}\frac{U_{i+\frac{1}{2}}^{n+1}-U_{i-\frac{1}{2}}^n}{\Delta t}+g\,\frac{\eta_{i+1}^{n+1}-\eta_i^{n+1}}{\Delta x}+f\frac{\omega}{n}U_{i+\frac{1}{2}}^{n+1}=0, \quad (20)$$

where $q=hu$ and $Q=HU$ denoting mass flux along the upper and lower layer, respectively. In this staggered scheme, the values of η are computed at every full grid points x_i, with i=1,2,...,Nx, whereas velocity u,U are computed at every staggered grid points $x_{i+\frac{1}{2}}$, with i=1,2,...,Nx+1. In equation (18), values of $q_{i+\frac{1}{2}}$ and $Q_{i+\frac{1}{2}}$ depend on $h_{i+1/2}$ and $H_{i+1/2}$ which are unknown, and we indicate them with *. We use the first order upwind method to approximate them as follows:

$$^*h_{i+1/2}=\begin{cases} h_i, \ if \ \ u_{i+1/2}>0 \\ h_{i+1}, if \ \ u_{i+\frac{1}{2}}\le 0, \end{cases} \quad (21)$$

$$^*H_{i+1/2}=\begin{cases} H_i, if \ \ U_{i+\frac{1}{2}}>0 \\ H_{i+1}, if \ \ U_{i+1/2}\le 0, \end{cases}$$

When the flow is going to the right $u_{i+1/2}>0$ the above approximation gives $h_i u_{i+1/2}$ as the mass flux across $x_{i+1/2}$ for the upper layer and $\frac{1}{n}H_i U_{i+1/2}$ for the lower layer. By doing this, we maintain mass conservation in each cell A_i,i=1,2,..,Nx.

Hydrodynamic Pressure:

In an attempt to include the effect of vertical acceleration, we need to consider the full set of equations (9-14). First, we consider the fact that hydrodynamic pressure is zero at the surface $P(x, z=\eta(x,t), t)=0$ and it is increasing with depth. Here we assume P to be linearly dependent on z.

In the discrete hydrostatic model as explained previously, η are computed at full grid points x_i, whereas u and U are computed at half grid points $x_{i+\frac{1}{2}}$. In this hydrodynamic model, variables w,W, and P are all calculated at full grid points x_i. This grid arrangement is depicted in Figure 3. Let P_i denotes the pressure along the impermeable bottom $z=-d_1$ at grid x_i. Based on that assumption P is almost constant in the lower layer, thus P along the interface $z=-d_2$ is similar pressure at the bottom P_i. Note that in this setting we only need one vector array for dynamic pressure P_i^n and two vector arrays for w_i^n and W_i^n. Compare with solving the full 2D problem, this numerical scheme is much more efficient. And yet we show later that this two layer approximation already give good results.

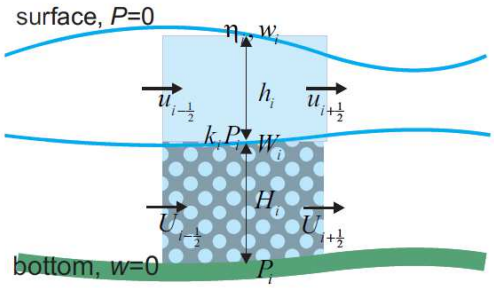

Fig.3: Illustration of hydrodynamic discrete model with positions for discrete variables.

In this two layer approach, hydrodynamic correction is formulated below. Suppose at any time step, we have calculated $\eta_i^{n+1}, \bar{u}, \bar{U}$, and $\bar{w}, \bar{W}$ from the hydrostatic model (18-20). Variables with bars indicates that they need corrections from the hydrodynamic terms. Correction for horizontal and vertical velocity components are calculated as follows:

$$u_{i+\frac{1}{2}}^{n+1} = \bar{u}_{i+1/2} - \frac{\Delta t}{2\Delta x}(P_{i+1}^{n+1} - P_i^{n+1}), \quad (23)$$

$$U_{i+\frac{1}{2}}^{n+1} = \bar{U}_{i+1/2} - \frac{\Delta t}{\Delta x}(P_{i+1}^{n+1} - P_i^{n+1}), \quad (24)$$

$$w_i^{n+1} = \overline{w_i} + \frac{\Delta t}{h_i^{n+1}} P_i^{n+1}, \quad (25)$$

$$W_i^{n+1} = \overline{W_i} + \frac{\Delta t}{H_i^{n+1}} P_i^{n+1}. \quad (26)$$

In all formulas above, values of P_i^{n+1} are needed, and hence we need to calculate P_i^{n+1} first. A way to do that is discussed below. Continuity equation (10) can be approximated as

$$w + (hu)_x + \frac{1}{n}(HU)_x = 0, \quad (27)$$

after implementing $\eta_t = w$ which is the linearized kinetic boundary condition (7). Further, mass conservation in the lower layer reads as

$$\frac{1}{n}W + \frac{1}{n}(HU)_x = 0 \quad (28)$$

Adding (27) and (28) yields

$$w + \frac{1}{n}W + (hu)_x + \frac{2}{n}(HU)_x = 0 \quad (29)$$

and its discrete counter parts is

$$w_i^{n+1} + \frac{1}{n}W_i^{n+1} + h_i^{n+1}\frac{u_{i+\frac{1}{2}}^{n+1} - u_{i-\frac{1}{2}}^{n+1}}{\Delta x} + \frac{2}{n}H_i^{n+1}\frac{U_{i+\frac{1}{2}}^{n+1} - U_{i-\frac{1}{2}}^{n+1}}{\Delta x} = 0. \quad (30)$$

Substituting the correction (23-26) into (30) give us a tridiagonal system of equations for P_i^{n+1}.

Finally, the computational procedure in the hydrodynamic scheme is as follows:

1. Solving the tridiagonal system (30) for P^{n+1} by means of Thomas algorithm.
2. Make correction for u^{n+1} and U^{n+1} by substituting P^{n+1} into equations (23) and (24), respectively.
3. Make correction for w^{n+1}, W^{n+1} by substituting P^{n+1} into equations (25) and (26).

Wave Damping By A Porous Media:

In the propagation of wave over a porous breakwater, damping effect is observed due to interaction between fluid and the porous structure. Here we implement the hydrodynamic scheme to simulate wave propagates overa porous structure.

For simulation of an incoming monochromatic wave passing over a submerged porous breakwater, we take a zero initial condition $\eta(x,0) = u(x,0) = U(x,0) = 0$ and the left influx monochromatic wave $\eta(x,t) = asin\omega t$ with amplitude a=0.5 and frequency$\omega = 1$. Along the right boundary, we implement an absorbing boundary by applying the sponge layer technique. For computation we use parameters d_1=10, d_2=20, n=0.7, f=0.25, and g=9.81. The numerical results of incoming monochromatic wave passing over a submerged porous breakwater are given in Figure 4. Simulation result clearly shows that the wave amplitude is reduced.

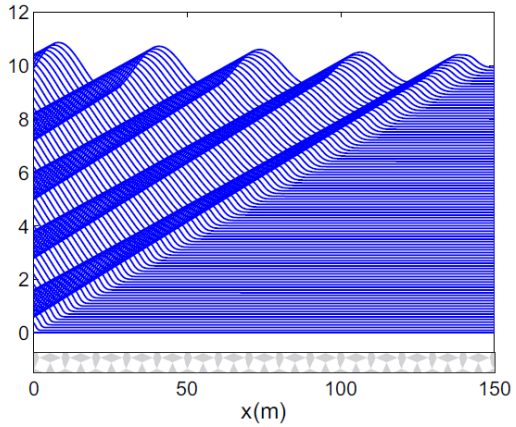

Fig.4: Amplitude of incoming monochromatic wave reduces over a submerged porous breakwater.

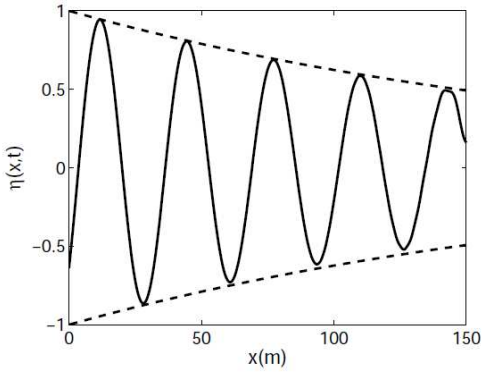

Fig.5: Comparison between numerical (line) with analytical result (dash).

Further, we show that the numerical wave profile reduces by the porous media has an envelope that confirms the analytical damping. Dispersion relation for free surface flow over a submerged porous medium is

$$\frac{\omega^2}{gk} = \frac{n\tanh k(d_1-d_2)+\alpha\tanh kd_1}{n\tanh kd_1\tanh k(d_2-d_1)+\alpha} \qquad (31)$$

with $\alpha = (1 - if)$. For the detail derivation, see (Pudjaprasetya, S., and I. Magdalena, 2013) and (Tsai, C., H. Chen and F. Lee, 2006). Using parameter values above, dispersion relation (31) results in a complex value wave number k=0.1055156400-0.004724311893 I. The negative sign of the imaginary part k of the monochromatic wave $e^{i(kx-\omega t)}$ corresponds to amplitude reduction with an envelope $|e^{i(kx-\omega t)}|$. Figure 5 displays the analytical curve of $|e^{i(kx-\omega t)}|$ together with numerical surface elevation. Clearly, the reduction of numerical surface amplitude confirms the analytical damping.

Standing Wave Reduces Over A Porous Media:

In this section, we compare the numerical amplitude reduction with experimental data. We use the experimental data of an oscillating standing waves over porous bottom as recorded in (Gu, Z., and H. Wang, 1991).

The experiment was conducted in a closed basin with length $L = 200\,cm$ and water depth $d_2 = 45\,cm$. Along thebottom,a layerofporousmediumheight15 cm, is filled with river gravel diameter $D_{50} = 1.48\,cm$, and porosity of this medium is $n = 0.359$. Initially, a standing wave with amplitude$A = 0.0295\,cm$and wave length$k = \frac{2\pi}{L}$, is generated in the wave flume using a piston type wave maker. Astimeprogressesthe amplitude of the standing wavereduces.The standing wave amplitude as a function of time is measured by wave gauges in the middle of the basin.

For comparison with the experimental data, we use the hydrodynamic scheme with full non-linear friction$(\alpha + \beta|U|)U$.Notation αdenotes the laminar friction and βturbulent friction. Empirical formulas as suggested by (Engelund F., 1953)for the laminar and turbulent friction coefficients are

$$\alpha = \frac{\alpha_0(1-n)^3\nu}{n^2 D_{50}}, \beta = \frac{\beta_0(1-n)}{n^3 D_{50}} \qquad (32)$$

with $\alpha_0$and $\beta_0$are the Dupuit-Forchheimer constants, $D_{50}$is adiameter ofporous material, and νiskinematic viscosity.The computations useΔx=0.01,Δt =0.001, and g =9.81. Parameters for friction are $\nu = 0.05, \alpha_0 = 570, \beta = 3$.

Australian Journal of Basic and Applied Sciences, 9(28) Special 2015, Pages: 124-130

The initial standing wave is generated by implementing initial wave $\eta(x,0) = A\cos kx$, with left and right hard wall boundary conditions. In the middle of the wave basin, at x_p=L/2, the wave height is recorded as a function of time $\eta\left(x_p = \frac{L}{2}, t\right)$ and the result is given in Figure 6 (top). As time progresses, the wave undergo amplitude reduction. Further, we calculate the normalized wave height $\frac{|\eta|}{A}$from the previous numerical simulation, and in Figure 6 (bottom) we plot the numerical result together with the experimental data. Clearly, they show a good agreement. Apart from agreement in wave attenuation. Figure 6 (top) displays that our hydrodynamic scheme can produce the correct wave speed especially during finite time. Agreement in the wave speed means that the scheme can produce correct dispersion. We note that a calculation without hydrodynamic term will not give correct dispersion and wave damping, see Figure 7.

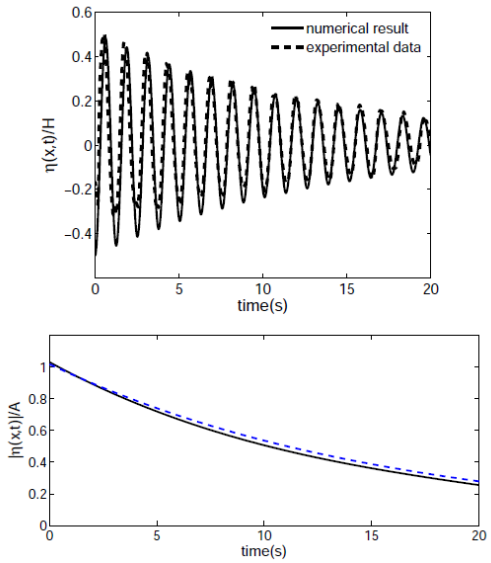

Fig. 6: Comparison between numerical result (line) with experimental data (dash). (Top) Normalized surface elevation $\frac{\eta(x_p=100cm,t)}{H}$. (Bottom) the non-dimensional wave height $\frac{|\eta|}{A}$.

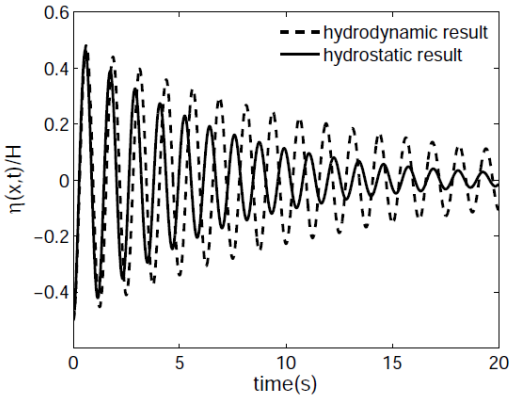

Fig. 7: Significant difference in wave attenuation calculated using hydrostatic (solid line) with hydrodynamic result (dashed line) models.

Conclusions:

We have presented a numerical method for calculating free surface flow over a submerged porous media. The equations used are the two layers of shallow water model, with Darcy resistance in the momentum equation for flow in a porous media. The scheme approximates the hydrodynamic pressure gradients, and produces accurate numerical solutions. The reduction of the numerical wave amplitude is shown to follow the analytical damping. A comparison with experimental data from (Gu, Z., and H. Wang, 1991)was conducted for standing waves over porous media. Our hydrodynamic scheme results in a wave that propagates with the correct speed, showing a good agreement with the experiment.

ACKNOWLEDGMENTS

Authors wishing to acknowledge the support of the Ensemble Estimation of Flood Risk in a Changing Climate project funded by The British Council through their Global InnovationInitiative.Desentralisasi ITB 2015: 311n/l1.C01/P/2015 is also acknowledged.

REFERENCES

Casulli, V., 1999. A semi-implicit finite difference method for non-hydrostatic free surface flows. International Journal for Numerical Methods in Fluids, 30(4): 425–440.

Cruz, E., M.Isobe and Watanabe, 1997. A. Boussinesq equations for wave transformation on porous bed. Coastal Enggineering, 30: 125-156.

DO, K., and K.SUH, Wavedampingover a multilayered,permeable seabed. Journal of Coastal Research, 6 (27): 1183-1190.

Engelund, F., 1953. On the laminar and turbulent flows of ground water through homogeneous sand. Transaction of The Danish Academy of Technical Sciences, 3: 4.

Gu, Z., and H.Wang, 1991. Gravity waves over porous bottoms. Coastal Engineering, 15: 497-524.

Magdalena, I., S.Pudjaprasetya and L.Wiryanto, Wave interaction with an emerged porous media. Advances in Applied Mathematics and Mechanics 6(5) : 680-692.

Nwogu, O., and Z.Demirbilek, 2006. Nonlinear wave interaction with submerged and surface-piercing porous structures. Coastal Engineering Conference, 1: 287-299.

Pudjaprasetya, S., and I.Magdalena, 2013. Wave energy dissipation over porous media. Applied Mathematical Sciences, 7(59): 2925-2937.

Pudjaprasetya, S., and I.Magdalena, 2014. Momentum conservative scheme for dam break and wave run up simulations. East Asia Journal on Applied Mathematics.

Stelling, G., and S.Duinmeijer, 2003. A staggered conservative scheme for every Froude number in rapidly varied shallow water flows. International Journal for Numerical Methods in Fluids., 43: 1329-1354.

Stelling, G., and M.Zijlema, 2003. An accurate and efficient finite-difference algorithm for non-hydrostatic free-surface flow with application to wave propagation. International Journal for Numerical Methods in Fluids, 1-23.

Tsai, C., H.Chen and F.Lee, 2006. Wave transformation over submerged permeable breakwater on porous bottom. Ocean Engineering, 33: 1623-1643.

Yamazaki, Y., K.Cheung and Z.Kowalik, 2011. Depth-integrated, non-hydrostatic model with grid nesting for tsunami generation, propagation, and run-up. International Journal for Numerical Methods in Fluids, 67: 2081-2107.

Zijlema, M., and G.Stelling, 2008. Efficient computation of surf zone waves using the nonlinear shallow water equations with non-hydrostatic pressure. Coastal Engineering, 55(10): 780-790.